Solid krypton: Equation of state and elastic properties

A. Polian and J. M. Besson
Physique des Milieux Condensés, Université Pierre et Marie Curie, Tour 13, Etage 4, 4 place Jussieu, F-75252 Paris CEDEX 05, France

M. Grimsditch
Materials Science Division, Argonne National Laboratory, Argonne, Illinios 60439

W. A. Grosshans
Universität GH Paderborn–Fachbereich Physik, Warburgerstrasse 100, D-4790 Paderborn, Federal Republic of Germany

(Received 6 June 1988)

The properties of solid krypton have been measured as a function of pressure in a diamond-anvil cell using energy-dispersive x-ray diffraction and Brillouin scattering. A room-temperature equation of state and a complete set of elastic constants are deduced. The analysis of these results indicates a possible phase transition above 30 GPa.

I. INTRODUCTION

Because of their simple electronic configurations, rare-gas solids are the best candidates for model calculations. It is only relatively recently, however, that the properties of these solids have been measured to very high pressure and hence made it possible to test theoretical predictions in this domain. Most work to date has concentrated on helium, argon, and xenon, while neon and krypton have received considerably less attention.

In the present paper we present the room-temperature equation of state (EOS) of krypton measured by x-ray energy-dispersive techniques using synchrotron radiation and the elastic properties determined using Brillouin scattering. From our results we conclude that the fcc phase may not be the most stable phase at high pressures.

In Sec. II we briefly review the techniques of energy-dispersive x-ray diffraction and of Brillouin scattering. The experimental results are presented and discussed in Sec. III and our conclusions are summarized in Sec. IV.

II. EXPERIMENTAL

A. Energy-dispersive x-ray diffraction

The experiments were performed at Hamburger Synchrotronstrahlungslabor (HASYLAB), Deutsches Elektronen-Synchrotron (DESY), in Hamburg, using a spectrometer which allows simultaneous recording of x-ray diffraction and ruby luminescence spectra.[1] The main parts of such a spectrometer are (a) collimators for the incident and the scattered x-ray beams which define the diffraction angle 2θ; (b) a solid-state detector with a multichannel pulse height analyzer; and (c) an optical spectrometer for the detection of the ruby luminescence.

In a given run, we were able to follow between three and seven krypton diffraction lines, depending on the particular orientations of the crystallites in our cell. In some runs, the (200) Kr line is hidden by a diffraction line from the Inconel gasket. We have not performed a uniaxial stress analysis[2] of our results because krypton is a gas at room temperature and we do not have a zero-pressure calibration, and also because the relatively small number of observed lines makes such an analysis subject to large errors.

The accumulation time was approximately 15 min at each pressure. The diamond anvil cell (DAC) used in these experiments was the Syassen-Holzapfel type.[3] The cell was loaded by condensing krypton on the gasket of the cell cooled in liquid nitrogen. After compression, the krypton thus produced is polycrystalline enough to allow the energy-dispersive x-ray (EDX) technique to be used.

B. Brillouin scattering

The Brillouin-scattering experiments were performed using a five-pass Fabry-Pérot interferometer and 200 mW of 514.5-nm radiation from a single-mode argon laser. The DAC used in these experiments was of Block-Piermarini type,[4] which allows only the backscattering geometry to be used. In this geometry the Brillouin frequency shift ($\Delta\sigma$) (in wave numbers) is given by

$$\Delta\sigma = \frac{2nv}{\lambda c} , \tag{1}$$

where n is the refractive index, v the sound velocity, λ the wavelength of incident radiation, and c the velocity of light. The free spectral range (FSR) of the interferometer is chosen so that the very intense Brillouin peaks from the diamond anvils are hidden in the unshifted laser line. Loading of this DAC is made in the same way as reported for argon.[5] Single crystals are obtained in the same way as previously described for H_2O.[6] In both x-ray and Brillouin experiments, the pressure was measured using the nonlinear ruby fluorescence scale.[7]

III. RESULTS AND DISCUSSION

A. X-ray diffraction

Examples of EDX spectra of krypton at various pressures are shown in Fig. 1. The shifts of the diffraction peaks with pressure are easily seen. These spectra yield the spacing d_{hkl} between the (hkl) planes from which the lattice parameter is calculated assuming cubic symmetry. The density is then calculated from the lattice constant.

Fits with the Keane or with the Murnaghan equation of state (EOS) gave similar results, so we have chosen to fit the pressure dependence of the density with a first-order Murnaghan EOS, viz.,

$$\rho=\rho_0\left[1+\frac{B'P}{B_0}\right]^{1/B'}, \tag{2}$$

where ρ is the density and P the pressure. B and B' are the bulk modulus and its first derivative with respect to pressure, and a subscript 0 indicates quantities at $P=0$. Although a least-squares fit to the data yields $\rho_0=2.317$ g/cm^3, $B_0=1.41$ GPa, and $B'=4.3\pm0.1$, the values of ρ_0 and B_0 are not well defined. A fit with $\rho_0=2.8$ g/cm^3 and $B_0=3.6$ GPa and another fit with $\rho_0=0.1$ g/cm^3 and $B_0=1.2\times10^{-6}$ GPa both yield values, in the pressure range 2–30 GPa, that differ by less than 0.06 g/cm^3 (roughly the experimental error) from the best-fit values. Our experimental results are shown in Fig. 2 (points) together with the recent measurements of Alexandrov *et al.*[8] (crosses) and the fit (solid line). Moreover, our experimental results are also presented in Table I so as to facilitate comparisons with future theoretical calculations.

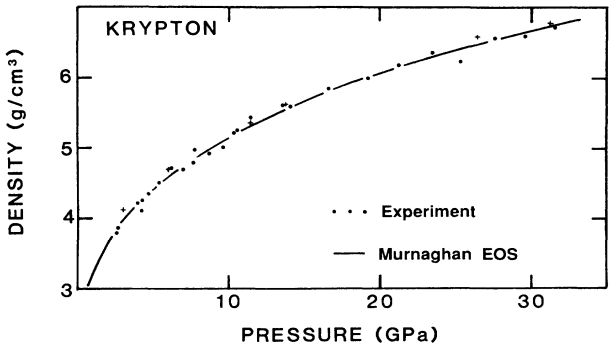

FIG. 2. Experimental (points) and calculated (line) equation of state of solid krypton. The crosses are taken from Ref. 8.

At this point, we want to note that comparisons between the experimental EOS and calculated ones[9] show that, as for argon,[5] three-body exchange interaction effects are important, i.e., calculations based only on pair potentials are not sufficient to describe the density and the elastic properties of solid rare gases.

B. Brillouin scattering

In Fig. 3 we present the measured Brillouin frequency shift of krypton as a function of pressure. Using Eq. (1),

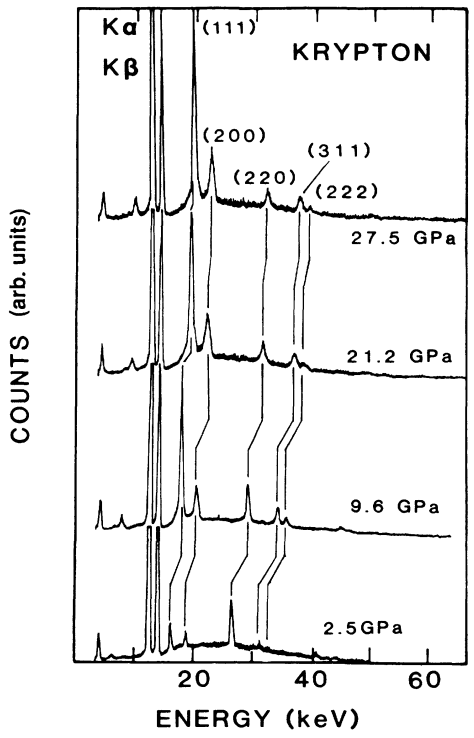

FIG. 1. Diffraction spectra at various pressures show the shift of the various diffraction lines.

TABLE I. Experimental results for the density as a function of pressure. Estimated errors are 0.06 g/cm^3.

P (GPa)	ρ (g/cm^3)
2.53	3.78
2.61	3.88
3.97	4.23
4.22	4.11
4.25	4.26
4.62	4.46
5.68	4.51
6.13	4.72
6.96	4.71
7.72	4.98
7.73	4.80
8.76	4.93
9.64	5.01
10.33	5.24
10.62	5.26
11.43	5.45
13.54	5.61
14.15	5.61
16.6	5.85
19.2	6.01
21.3	6.18
23.5	6.37
25.2	6.26
27.6	6.57
29.6	6.60
31.6	6.72

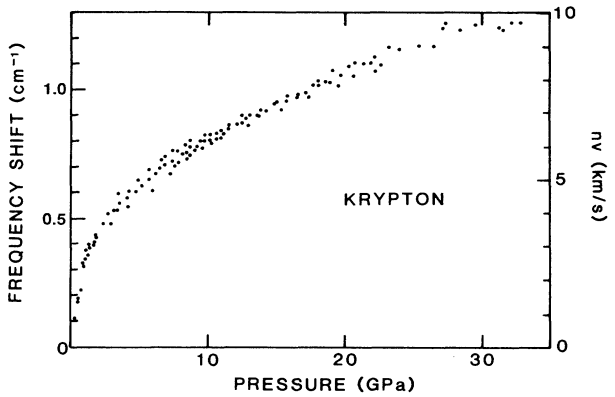

FIG. 3. Brillouin shift in cm^{-1} (left-hand scale) and corresponding nv product in km/s (right-hand scale) as a function of pressure. The four points at the lowest pressure are in the fluid phase.

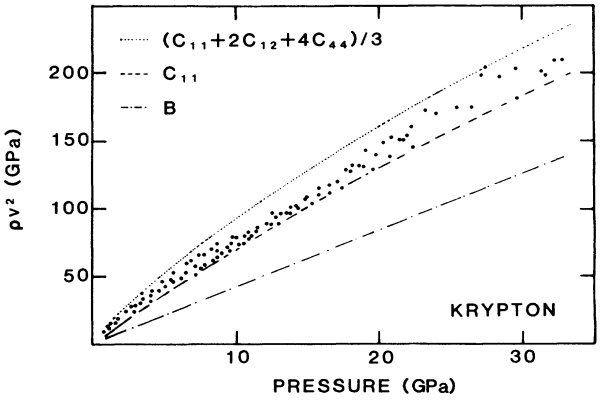

FIG. 5. Experimental elastic moduli ρv^2 in GPa (points) of krypton as a function of pressure. The two envelope curves (dotted and dashed lines) represent $C_{\max}=\frac{1}{3}(C_{11}+2C_{12}+4C_{44})$ and C_{11}, respectively. The bulk modulus (dotted-dashed line) is also represented.

we obtain the values of nv shown on the right-hand side of Fig. 3. In this figure, the freezing point at 0.75 GPa is clearly seen. Since in our DAC we could not maintain krypton below 0.3 GPa, we do not have enough data to make meaningful calculations and fits in the fluid region. In the solid phase on the other hand, we have many experimental points. The experiments were done either on single crystals, obtained in the same manner as previously described for H_2O (Refs. 6 and 10) or on polycrystals. As already pointed out in the case of argon,[5,11] when one pressurizes single crystals of krypton, recrystallization sometimes occurs in the cell, so that, by Brillouin scattering, one measures the sound velocity along various crystalline orientations. This explains the spread of the experimental points even when single crystals are formed at the freezing point.

As shown by Eq. (1), in order to deduce the sound velocity from Brillouin-scattering measurements, it is necessary to know the refractive index, and in the present case its variation with pressure. Such measurements have recently been shown to be possible[12] but have not yet been performed for krypton. However, since it is known[13] that for compounds which are described by the same functional form of the interatomic potential a law of corresponding states exists by means of which the properties of one may be deduced from those of another one, we obtain the refractive index of krypton from that of xenon[13] using

$$\frac{n^2-1}{n^2+2}=\frac{3.304}{\left[\dfrac{5.4}{E_b^2-E^2}+2.5\times10^{-4}\right]}\rho\ , \tag{3}$$

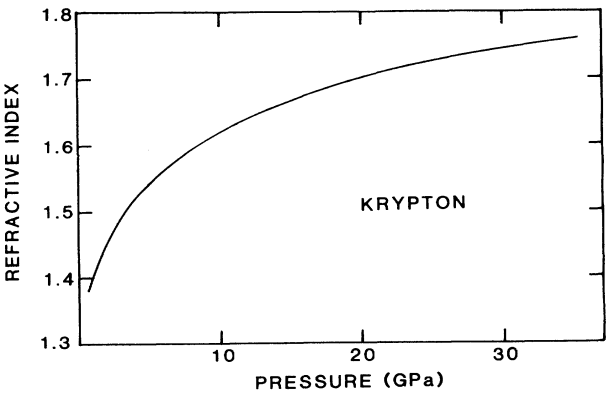

FIG. 4. Refractive index of krypton deduced from that of xenon (see text) as a function of pressure.

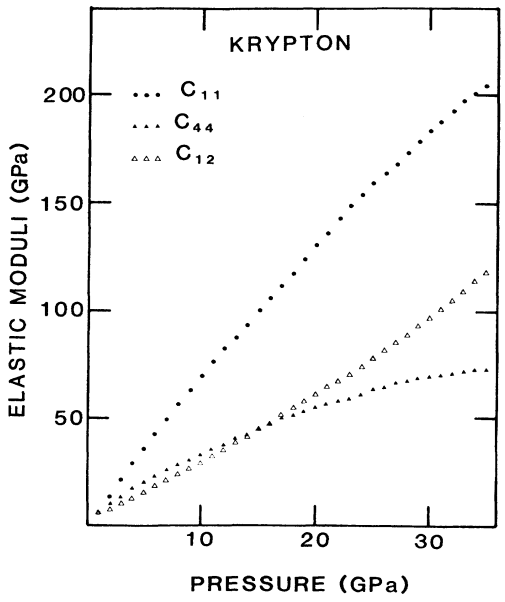

FIG. 6. Elastic constants (GPa) of krypton as a function of pressure.

where

$$E_b = 15.46 + 0.381(0.5234\rho - 1)^{1.8} \text{ eV} , \quad (4)$$

and E is the photon energy at which the refractive index is calculated. E and E_b are in eV and ρ in g/cm^3. The refractive index obtained from Eqs. (3) and (4) is shown in Fig. 4. In spite of the fact that the above derivation of the refractive index may contain systematic errors up to a few percent, they do not affect the general conclusions regarding the elastic properties, which we draw in the following paragraphs.

The sound velocity is related to an effective elastic constant C through

$$C = \rho v^2 , \quad (5)$$

where ρ is the density. In general, C is a function of many elements of the elastic constant tensor. In the present case, because the phonon propagation direction is not known in the reference frame of the crystal, the exact combination cannot be determined.

Using the Brillouin-scattering results (Fig. 3) the calculated refractive index (Fig. 4) and the density (Fig. 2), we determine the effective elastic constants shown in Fig. 5 (dots). The spread of the experimental points is due to the spread of the measured frequency shift (Fig. 3) which in turn is due to having probed different crystallographic orientations in different runs. This spread in our results can be used to our advantage: in cubic crystals, it is well known[14] that the extrema of the longitudinal elastic moduli are C_{11} (in the [100] direction) and $C^* = \frac{1}{3}(C_{11} + 2C_{12} + 4C_{44})$ (in the [111] direction). From low-temperature measurements[15] it is known that the elastic moduli of rare-gas solids are minima along the [100] directions (C_{11}) and maxima along the [111] directions (C^*). In Fig. 5 we therefore plot the envelope curves of the experimental points. The upper one (dotted line) can be taken as a lower limit of C^* and the lower one (dashed line) as an upper limit of C_{11}. Given the

TABLE II. Experimental and elastic constants of solid Kr as a function of pressure. (All quantities in GPa.)

P	$C_{\min} = C_{11}$	$C_{\max} = C^*$	B	C_{12}	C_{44}
1	6±2	14±2	6±2	6±4	6±3
2	14±2	24±2	10±2	8±4	11±3
3	22±2	33±2	14±2	10±4	14±3
4	30±2	42±2	18±2	12±4	18±3
5	36±2	51±2	23±2	17±4	21±3
6	43±2	58±3	27±2	19±4	23±4
7	50±2	66±3	31±2	22±4	26±4
8	57±2	73±3	35±2	24±4	29±4
9	64±2	81±3	39±2	27±5	32±4
10	71±2	88±3	43±2	29±5	34±4
11	77±2	96±4	47±3	32±5	37±4
12	83±2	103±4	52±3	37±5	38±5
13	89±2	110±4	56±3	40±5	41±5
14	94±2	117±4	60±3	43±5	43±5
15	101±2	124±4	64±3	46±6	45±5
16	107±2	132±4	68±3	49±6	48±5
17	112±2	140±4	72±3	52±6	51±5
18	118±2	146±4	76±3	55±6	53±5
19	125±2	152±4	81±3	59±6	53±5
20	131±2	159±4	85±3	62±6	56±5
21	137±2	165±4	89±3	65±6	57±5
22	144±2	171±4	93±3	68±7	59±5
23	149±2	177±4	97±3	71±7	60±5
24	154±3	184±4	101±4	75±7	62±6
25	160±3	191±4	106±4	79±7	64±6
26	165±3	197±4	110±4	83±7	65±6
27	169±3	203±4	114±4	87±7	67±6
28	174±3	208±4	118±4	90±7	68±6
29	179±3	214±4	122±4	94±7	69±6
30	184±3	219±4	126±4	97±8	70±6
31	189±3	225±4	130±4	101±8	71±6
32	194±3	230±4	135±4	106±8	71±6
33	198±3	235±4	139±4	110±8	72±6
34	201±3	240±4	143±4	114±8	73±6
35	205±3	244±4	147±4	118±8	73±6

large number of data points, we are reasonably sure of having probed almost all crystallographic directions, therefore the envelope curves should be exactly C_{11} and C^*.

On the same figure we have also plotted (dashed-dotted line) the adiabatic bulk modulus B obtained from our density fit. In a cubic crystal we have

$$B=\tfrac{1}{3}(C_{11}+2C_{12}) . \quad (6)$$

We assume that C_{11} and C^* are indeed given by the envelope curves in Fig. 5. In that case, from C_{11}, C^*, and B, we deduce the complete set of elastic constants shown in Fig. 6 and listed in Table II.

Given the uncertainties in C_{11} and C^* discussed above, it is easy to see that the C_{ij} given in Fig. 6 are upper limits for C_{11} and lower bounds for C_{44} and C_{12}. The overall behavior with pressure, however, is not expected to be changed much by these considerations. Of particular interest is the behavior of C_{11} and C_{12}; as can be seen in Fig. 6, if the trend in these two constants is extrapolated to higher pressures, at some higher pressure they will become equal, thus violating one of the stability conditions for a cubic material (viz., $C_{11}-C_{12}>0$). This is an indication that at higher pressures the fcc phase of Kr may not be stable but could transform into a different structure. Such a phase transition, predicted by calculations,[9] has already been observed in solid xenon by x-ray diffraction.[16]

In a previous article in which we discussed the elastic properties of argon,[5] we were able to further interpret our results to yield values for the elastic anisotropy $[2C_{44}/(C_{11}-C_{12})]$ and the deviations (δ) from the Cauchy condition

$$\delta=(C_{44}-C_{12}+2P)/C_{12} . \quad (7)$$

In the present case, because of the larger errors in the elastic constants (especially in B), these evaluations are practically meaningless since at low pressures the errors in δ are larger than δ itself. However, it is known from low-temperature results at one atmosphere[15] that the Cauchy relationship is well satisfied. From our results, on the other hand, we find that for $P\gtrsim 10$ GPa $\delta\neq 0$, showing that as the pressure is increased, the Cauchy condition is less well satisfied, and indicating in turn that in order to accurately calculate the elastic constants of krypton, a model with noncentral or many-body forces must be employed.

IV. CONCLUSION

In this paper, we have presented results on the equation of state of solid krypton, obtained by energy-dispersive x-ray diffraction using synchrotron radiation, and its elastic properties determined by Brillouin scattering. Taking advantage of the fact that single crystals of krypton change their orientations with respect to the optical axis of the cell as a function of pressure, we have been able to measure a large number of orientations, which allows us to deduce limits for all the elastic constants. The analysis of these results indicates that the fcc phase of rare-gas solids may not be stable at very high pressures.

ACKNOWLEDGMENTS

This work was supported by the Institut National d'Astronomie et de Geophysique under Grant No. 83.70978, the Commissariat a l'Energie Atomique under Grant No. 1617-A4, the U.S. Department of Energy, BES-Materials Sciences, under Contract No. W-31-109-ENG-38, and the German Ministry of Research and Technology under Contract No. 05 340 AxB0. Helpful discussions with P. Loubeyre and technical assistance of B. Lavernhe are gratefully acknowledged. The work of M.G. was performed while visiting the Laboratoire des Milieux Condenses. Physique des Milieux Condensés is a unité associeé au Centre National de la Recherche Scientifique.

[1]W. A. Grosshans, E. F. Duesing, and W. B. Holzapfel, High Temp.–High Pressures **16**, 539 (1984).
[2]A. K. Singh and G. C. Kennedy, J. Appl. Phys. **45**, 4686 (1974).
[3]K. Syassen and W. B. Holzapfel, Europhys. Conf. Abstr. **1A**, 75 (1975).
[4]G. J. Piermarini, S. Block, J. D. Barnett, and R. A. Forman, J. Appl. Phys. **46**, 2774 (1975).
[5]M. Grimsditch, P. Loubeyre, and A. Polian, Phys. Rev. B **33**, 7192 (1986).
[6]A. Polian and M. Grimsditch, Phys. Rev. Lett. **52**, 1312 (1984).
[7]H. K. Mao, P. M. Bell, J. W. Shaner, and D. J. Steinberg, J. Appl. Phys. **49**, 3276 (1978).
[8]I. V. Alexandrov, A. N. Zisman, and S. M. Stishov, Zh. Eksp. Teor. Fiz. **65**, 371 (1987) [Sov. Phys.—JETP **92**, 657 (1987)].
[9]P. Loubeyre, unpublished.
[10]A. Polian and M. Grimsditch, Phys. Rev. B **27**, 6409 (1983).
[11]P. M. Bell and H. K. Mao, Carnegie Inst. Washington Yearb. **80**, 404 (1981).
[12]M. Grimsditch, R. LeToullec, A. Polian, and M. Gauthier, J. Appl. Phys. **60**, 3479 (1986).
[13]J. P. Itie, these troisième cycle, Université Pierre et Marie Curie, Paris, 1984 (unpublished); J. P. Itie and R. LeToullec, J. Phys. (Paris) Colloq. **45**, C8-53 (1984).
[14]See, for instance, H. Z. Cummins and P. E. Schoen, in *Laser Handbook,* edited by F. T. Arecchi and E. O. Schulz-Dubois (North-Holland, Amsterdam, 1972), p. 1029.
[15]B. P. Stoicheff, in *Rare Gas Solids,* edited by J. A. Venobles and M. L. Klein (Academic, New York, 1976), p. 979.
[16]A. P. Jephcoat, H. K. Mao, L. W. Finger, D. E. Cox, R. J. Hemley, and C. S. Zha, Phys. Rev. Lett. **59**, 2670 (1987).
[17]M. Born and K. Huang, *Dynamical Theory of Crystal Lattices* (Clarendon, Oxford, 1954), p. 129.